Eur Biophys J (2011) 40:195–208
DOI 10.1007/s00249-010-0639-2

ORIGINAL PAPER

Redox regulation of morphology, cell stiffness, and lectin-induced aggregation of human platelets

Ekaterina V. Shamova · Irina V. Gorudko · Elizaveta S. Drozd · Sergey A. Chizhik · Grigory G. Martinovich · Sergey N. Cherenkevich · Alexander V. Timoshenko

Received: 26 July 2010 / Revised: 11 October 2010 / Accepted: 20 October 2010 / Published online: 16 November 2010

Abstract Redox regulation and carbohydrate recognition are potent molecular mechanisms which can contribute to platelet aggregation in response to various stimuli. The purpose of this study is to investigate the relationship between these mechanisms and to examine whether cell surface glycocalyx and cell stiffness of human platelets are sensitive to the redox potential formed by glutathione. To this end, human platelets were treated with different concentrations (0.05 μM to 6 mM) and ratios of reduced or oxidized glutathione (GSH or GSSG), and platelet morphological, mechanical, and functional properties were determined using conventional light microscopy, atomic force microscopy, and lectin-induced cell aggregation analysis. It was found that lowering the glutathione redox potential changed platelet morphology and increased platelet stiffness as well as modulated nonuniformly platelet aggregation in response to plant lectins with different carbohydrate-binding specificity including wheat germ agglutinin, *Sambucus nigra* agglutinin, and *Canavalia ensiformis* agglutinin. Extracellular redox potential and redox buffering capacity of the GSSG/2GSH couple were shown to control the availability of specific lectin-binding glycoligands on the cell surface, while the intracellular glutathione redox state affected the general functional ability of platelets to be aggregated independently of the type of lectins. Our data provide the first experimental evidence that glutathione as a redox molecule can affect the mechanical stiffness of human platelets and induce changes of the cell surface glycocalyx, which may represent a new mechanism of redox regulation of intercellular contacts.

Keywords Aggregation · Cell stiffness · Glutathione · Human platelets · Lectins · Redox potential

Abbreviations

α-MM	α-Methyl-D-mannoside
Con A	*Canavalia ensiformis* agglutinin
DEM	Diethyl maleate
GlcNAc	*N*-acetyl-D-glucosamine
GSH	Reduced glutathione
GSSG	Oxidized glutathione
HSR	Haptenic-sugar-resistant
mBCl	Monochlorobimane
NEM	*N*-ethylmaleimide
PRP	Platelet-rich plasma
SNA	*Sambucus nigra* agglutinin
WGA	Wheat germ agglutinin
AFM	Atomic force microscopy

Introduction

Human platelets are small subcellular fragments of megakaryocytes which play a crucial role in hemostasis and maintaining vascular integrity. Platelets are very dynamic

Electronic supplementary material The online version of this article (doi:10.1007/s00249-010-0639-2) contains supplementary material, which is available to authorized users.

E. V. Shamova (✉) · I. V. Gorudko · G. G. Martinovich · S. N. Cherenkevich
Department of Biophysics, Belarusian State University, Nezavisimosti Ave. 4, 220030 Minsk, Belarus
e-mail: shamova@tut.by

E. S. Drozd · S. A. Chizhik
A.V. Luikov Institute of Heat and Mass Transfer, National Academy of Sciences of Belarus, P. Brovki St. 15, 220072 Minsk, Belarus

A. V. Timoshenko
Department of Biology, University of Western Ontario, London, ON N6G 5B7, Canada

structures and, upon activation, change their shape from small discs ($0.5 \times 3.0\ \mu m^2$) to more spherocytic cells with filopodia resulting from significant remodeling of the cytoskeleton (Hartwig 2006). These changes are associated with such important functions of platelets as adhesion to endothelium and aggregation, key events of primary hemostasis (Ruggeri 2002). Mechanical properties of human platelets might make a significant contribution to cell adhesion and aggregation, since cell stiffness was reported to influence strongly, for instance, the adhesiveness of human melanoma cells (Andre et al. 1990) and spreading of rat hepatocytes (Bhadriraju and Hansen 2002). Cell stiffness depends on the cytoskeleton state and can be very efficiently determined using atomic force microscopy (AFM) in both native and fixed conditions (Fritz et al. 1994; Radmacher et al. 1996; Yang et al. 2010).

There is strong evidence that platelet functions are regulated by glutathione, which makes these cells an excellent biophysical model to study mechanisms of redox control of cell aggregation (Essex 2009). Glutathione is available in the cell cytoplasm and whole blood at millimolar levels (Burch and Burch 1987; Hwang et al. 1992; Pastore et al. 2003), while at only micromolar levels in plasma (Pastore et al. 2003). Changes in intracellular and extracellular glutathione levels and in the ratio of its reduced (GSH) and oxidized (GSSG) forms often accompany diseases associated with concomitant impairment of platelet aggregation such as cardiovascular failure (Shimizu et al. 2004), diabetes (Samiec et al. 1998), and cancer (Kumar et al. 1995).

Depletion of intracellular glutathione in platelets by several compounds including diamide, *N*-ethylmaleimide (NEM), and quinones has been shown to correlate with inhibition of platelet aggregation (Matsuda et al. 1979; Hill et al. 1989; Samal et al. 1998; Kim et al. 2001). Exogenously added glutathione has been reported to modulate platelet aggregation in a characteristic, dose-dependent manner; i.e., platelet aggregation in response to conventional physiological agonists [adenosine diphosphate (ADP), collagen] was inhibited or enhanced depending on administration of high millimolar or low micromolar dosages of reduced glutathione (Pacchiarini et al. 1996; Essex and Li 2003). Surprisingly, at doses which enhance human platelet aggregation, glutathione has recently been shown to inhibit cell adhesion to immobilized fibronectin (Ball et al. 2008). Functional significance and molecular mechanisms of these controversial effects of glutathione remain uncertain, and at least two different approaches have been considered: first, a direct GSH-mediated biochemical modification of responsive signaling molecules, e.g., through glutathionylation (Ghezzi 2005), and, second, a redox-potential-dependent modification of functional responses of cells associated with the voltage of the environment as a biophysical factor. The latter mechanism is supported by data showing that lower extracellular redox potential is conducive to cell proliferation and T-cell activation (Jonas et al. 2002; Yan et al. 2009), while shifting the redox potential from a normal range of −(230–260) to −170 mV and more is associated with apoptosis, oxidative stress, and many diseases (Moriarty-Craige and Jones 2004; Palumaa 2009). Although $\alpha_{IIb}\beta_3$ integrin was reported to be a principal redox-sensitive adhesion protein of human platelets (Essex and Li 2003), the contribution of redox potential and redox buffering capacity of the GSSG/2GSH couple to regulation of platelet aggregation is still unclear, and it remains unknown whether these effects of glutathione are agonist specific.

Platelet activation and aggregation in most cases are governed through mobilization of glycoprotein receptors, which can be adequately probed by specific lectins, a type of multimeric carbohydrate-binding proteins. Lectins can recognize specific sugars of cell surface glycocalyx and cause clusterization of membrane glycoreceptors, transmembrane signaling, and cell aggregation similar to physiological agonists of platelets (Higashihara et al. 1985; Samal et al. 1998; Torti et al. 1999). Lectin-induced aggregation of cells has a very important technical advantage in comparison with physiological agonists, because this response can be specifically blocked by inhibiting haptenic sugars. If haptenic sugars are added to lectin-induced cell aggregates, nascent lectin bridges become disrupted and cannot be formed anymore, while any lectin-induced additional adhesive contacts remain stable and provide unique information about the stability of cell aggregates (Timoshenko et al. 1986, 1999; Gorudko et al. 2008). As much as lectins seem to be "crude" stimuli of platelet aggregation because they bind same sugar residues of different cell surface glycosylated molecules, the precise mechanisms of platelet activation and aggregation caused by lectins and physiological agonists may differ noticeably. For example, wheat germ agglutinin (WGA), a strong agonist of platelets, has been shown to elicit a prompt and sharp increase in platelet intracellular Ca^{2+} concentration, however in contrast to thrombin-mediated responses, this Ca^{2+} mobilization was sensitive to protein kinase inhibitor stausporine and was resistant to inhibition by cyclic adenosine monophosphate (AMP) (Yatomi et al. 1993). In comparison, efficient aggregation of platelets has been observed in response to *Sambucus nigra* agglutinin (SNA), which failed to affect intracellular Ca^{2+} availability (Samal et al. 1998). These differences in functional activity of lectins with different carbohydrate-binding specificity are central to their use as proper tools for studying platelet aggregation.

Since the platelet aggregation response in many aspects is determined by protein–carbohydrate interactions and is under control of redox systems, this study was designed to investigate effects of variable glutathione dosage on

aggregation of human platelets induced by plant lectins with different carbohydrate-binding activity as well as on morphology and stiffness of these cells. We also specifically addressed the biophysical question of whether extracellular redox potential and redox buffering capacity formed by the GSSG/2GSH couple is a regulatory factor of platelet aggregation.

Materials and methods

Reagents

Lectins including mannose/glucose-specific *Canavalia ensiformis* agglutinin (Con A), Neu5Acα(2,6)Gal/GalNAc-specific *Sambucus nigra* agglutinin (SNA), and GlcNAc-specific wheat germ agglutinin (WGA) were purchased from Lektinotest (Lviv, Ukraine). All other biochemicals were obtained from Sigma Aldrich (St. Louis, MO, USA) except for monochlorobimane (mBCl), which was obtained from Molecular Probes (Eugene, OR, USA), and reduced and oxidized glutathione, which were obtained from Applichem (Darmstadt, Germany).

Isolation of human platelets

All procedures of human platelet isolation were conducted at room temperature, and use of glass containers and pipettes was avoided. Venous blood samples were obtained from healthy donors at the Republic Scientific and Practical Centre of Hematology and Transfusion (Minsk, Belarus). Blood was collected in tubes containing 3.8% (w/v) trisodium citrate as anticoagulant at 9:1 ratio. To study ADP-induced platelet aggregation, platelet-rich plasma (PRP) was prepared by centrifugation of blood at $200 \times g$ for 10 min followed by cell counting and adjusting of cell concentration to 2.5×10^8 cells/ml in autologous blood plasma. To study lectin-induced platelet aggregation, washed platelets were prepared by additional two-step centrifugation of PRP at $600 \times g$ for 3 min at 20°C, and the cell pellet was resuspended in a Tris/ethylenediamine tetraacetic acid (EDTA) buffer solution (13.3 mM Tris, 120 mM NaCl, 15.4 mM KCl, 6 mM D-glucose, 1.5 mM EDTA, pH 6.9), with final cell concentration of 2.5×10^9 cells/ml. This buffer prevented self-aggregation and clumping of stored platelets in our experiments.

Measurement of platelet aggregation

The processes of platelet aggregation and disaggregation were measured at 37°C by light transmission using an analyzer of platelet aggregation (AP 2110; SOLAR, Minsk, Belarus). To study platelet aggregation, the aggregometer cuvette was filled with either 400 µl PRP or 50 µl washed platelets in Tris/EDTA storage buffer plus 350 µl phosphate-buffered saline (PBS) containing 1 mM $CaCl_2$ and 0.5 mM $MgCl_2$, and incubated at 37°C with stirring for 2 min (in the absence and presence of glutathione) before adding an agonist. Although our samples contained leftover EDTA, which is know to inhibit platelet aggregation at high concentration of 2 mM (Pidard et al. 1986), no EDTA-mediated inhibition was observed in our assays due to the relatively low EDTA concentration (only 0.19 mM) and the excess of Ca^{2+} and Mg^{2+} ions in the aggregating buffer.

ADP was used as a positive standard agonist and reference to plant lectins. Resistance of lectin-induced cell aggregates to dissociating action of haptenic sugars referred to as haptenic-sugar-resistant contacts (HSR contacts) was determined as described elsewhere (Timoshenko et al. 1986, 1999; Samal et al. 1998; Gorudko et al. 2008). In particular, to induce dissociation of cell aggregates, we used haptenic sugars at the following final concentrations: 100 mM GlcNAc, 60 mM lactose, and 60 mM α-methyl-D-mannoside (α-MM). For quantitative assessment of HSR contacts we used the parameter of stability R, which was calculated as $R = (T/T_0) \times 100\%$, where T is the steady-state value of light transmission after haptenic sugar addition and T_0 is the maximal value of light transmission reached during the process of platelet aggregation before adding the haptenic sugars.

Light microscopy

To confirm the formation of cell aggregates in response to lectins, microscopy analysis of cell samples, which were taken from the suspension of aggregating cells at plateau (maximal response), was performed. An aliquot of cells (100 µl) was mixed with an equal amount of 1.5% glutaraldehyde to fix cell aggregates and viewed using an optical microscope Olympus BX51W1 (Tokyo, Japan) and LUMPlanFl objective (40×/0.80). Images of cells and cell aggregates were captured using a digital camera (Olympus DP 20; Tokyo, Japan).

Investigation of platelet surface by atomic force microscopy

AFM is a unique technique which allows quantitative determination of microelastic properties of living cells in aqueous environment (Fritz et al. 1994; Radmacher et al. 1996) as well as fixed and dehydrated cells (Yang et al. 2010). In our study we used glutaraldehyde-fixed human platelets, which allowed avoidance of unwanted activation of platelets on glass slides (Radmacher et al. 1996) and detection of only sustained differences between GSH-treated and untreated cells.

PRP (200 µl at 2.5 × 10^8 cells/ml) was treated with GSH for 10 min at room temperature, fixed in 1.5% glutaraldehyde for 30 min, and centrifuged at 600 × *g* for 3 min. The supernatant was discarded, and the cell pellet was washed twice in PBS (10 mM Na_2HPO_4/KH_2PO_4, 137 mM NaCl, 2.7 mM KCl, pH 7.35) and twice in distilled water. Washed cells were put on a glass slide and dried in air for several hours. All steps were performed at room temperature.

AFM observations were carried out using a NT-206 microscope (MicroTestMachines, Minsk, Belarus) working in contact mode. Cantilevers (NSC11) with spring constant of 3 N/m were used. Tip radii were checked by using a standard TGT01 silicon grating from NT-MDT (Moscow, Russia) and were 40 nm for topography visualization and 100 nm for cell stiffness determination.

Local elastic properties of platelets were quantitatively determined using force spectroscopy regime. Force curves were obtained by recording cantilever deflection while the tip was brought into contact with a cell at a fixed point and retracted. Taking into account that the stiffness of human platelets varies significantly across the cell body (Fritz et al. 1994; Radmacher et al. 1996) and to avoid the influence of a rigid substrate on the magnitude of the estimating elasticity modulus (Mathur et al. 2001), we recorded at least three force curves only from the central region of five randomly selected cells for each treatment. The central region was characterized by the largest thickness within the body of fixed cells. The cell Young's moduli were calculated as described earlier (Chizhik et al. 1998; Drozd and Chizhik 2008) and used as a measure of platelet stiffness. Force curves as well as histograms of Young's modulus distribution at indentation depth of 25 nm are presented as Supplementary Data.

Calculation of extracellular redox potential of the GSSG/2GSH couple

The redox potential of the GSSG/2GSH redox couple was calculated according to the Nernst equation: $E_h = E_0 + (2.3RT/nF)\log([GSSG]/[GSH]^2)$, where $E_0 = -264$ mV at pH 7.4 (Kirlin et al. 1999), and $n = 2$. [GSH] is squared in this equation because two GSH molecules are needed to form one GSSG molecule. This means that not only the GSSG to GSH ratio but also the total concentration of glutathione determines the redox potential. In other words, a cellular environment with more total glutathione has a greater redox buffering capacity than one with lower glutathione level. Taking into account this notion and to analyze the role of redox potential, we maintained fixed glutathione concentration of 5 µM, 100 µM, 3 or 6 mM determined as total glutathione sulfur (GSH + 2GSSG) and varied the GSH to 2GSSG ratio in the range of 1:100 to 100:1.

Estimation of intracellular GSH level

Intracellular level of GSH was detected using mBCl assay as described elsewhere (Wang and Joseph 2000) with some modifications. Briefly, 50 µl platelet suspension (2.5 × 10^9 cells/ml) was added to 1.25 ml PBS supplemented with 0.2% Triton X-100 to lyse the cells, and then 80 µM mBCl together with 0.24 U/ml bovine glutathione S-transferase to increase the reaction rate between GSH and mBCl were added, leading to formation of highly fluorescent GSH-bimane adduct. The kinetics of fluorescence increase was recorded at 490 nm (excitation at 394 nm) using a LSF 1211A spectrofluorimeter (SOLAR). Steady-state fluorescence was typically achieved at 15 min and used for estimating the intracellular GSH level.

Statistical analysis

Data are presented as mean ± standard error of the mean (SEM); statistical significances between means were assayed using Student's *t* test. Correlation coefficients were determined using Pearson's test. Values of $P < 0.05$ were considered to indicate statistically significant differences.

Results and discussion

Aggregation response of GSH-treated human platelets depends on carbohydrate-binding specificity of plant lectins

Three lectins (WGA, Con A, and SNA) used in this study were selected based on their nonoverlapping carbohydrate-binding specificity (Sharon and Lis 2003). All these lectins were able to induce efficient aggregation of human platelets, which was detected as an increase in light transmission of cell suspensions and was comparable to the standard aggregation induced by ADP, our positive control (Fig. 1). Formation of true cell aggregates was further confirmed by microscopy analysis (Fig. 2). The lectin-induced aggregation was specifically blocked by corresponding haptenic sugars, i.e., by GlcNAc (WGA response), α-MM (Con A response), and lactose (SNA response) (Fig. 1). None of these sugars affected ADP-induced platelet aggregation, confirming the specificity of lectins as probes for cell surface glycoligands (data not shown). The differences in carbohydrate-binding specificity of lectins resulted in a rather unexpected variation of platelet aggregation observed in the presence of low (micromolar) concentrations of GSH. Thus, although GSH enhances in a dose-dependent manner (GSH concentrations range from 0.05 to 10 µM) platelet aggregation induced by ADP (2.5 µM), WGA (5 µg/ml), and Con A (10 µg/ml), the maximal fold increase of the cell

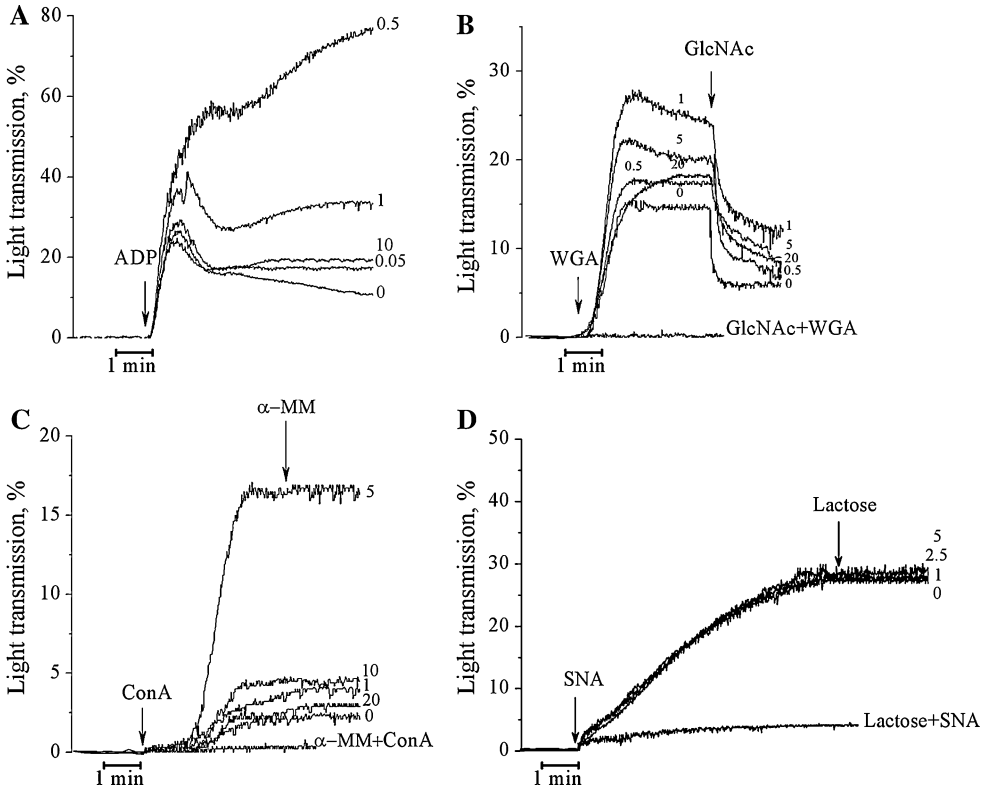

Fig. 1 Effect of GSH applied at low (micromolar) concentrations on platelet aggregation. Human platelets were treated with different concentrations of GSH as specified on the curves (0.05–20.0 μM) for 2 min before adding an aggregant: **a** 2.5 μM ADP, **b** 5 μg/ml WGA, **c** 10 μg/ml Con A, or **d** 75 μg/ml SNA. The *arrows* indicate the moment of adding agonists and haptenic sugars to the suspension of human platelets. When haptenic sugars were added before the lectins (shown as haptenic sugar + lectin), platelet aggregation did not occur. The haptenic sugars were used at concentrations of 100 mM GlcNAc, 60 mM α-MM, and 60 mM lactose. Typical kinetic curves of five independent experiments are presented

aggregation rate varied between these stimuli and was 2.4 ± 0.6, 1.4 ± 0.1, and 4.6 ± 1.2, respectively, which was consistent with microscopy observations (Fig. 2). All these effects were statistically significant in comparison with the aggregation of GSH-untreated cells ($n = 4$, $P < 0.05$). At the same time, GSH failed to affect platelet aggregation induced by SNA (75 μg/ml), which was relatively stable at the experimental conditions (Figs. 1, 2). These findings imply that GSH at low micromolar doses most likely potentiates platelet aggregation in conjunction with Ca^{2+}-mediated signaling, because the major functional difference between SNA and Con A/WGA is linked to their ability to affect intracellular free Ca^{2+}. All these three lectins have different carbohydrate-binding specificity, but only Con A and WGA induce an increase of cytoplasmic free Ca^{2+}, which is comparable to the thrombin and ADP responses (Samal et al. 1998). It should be noted that the stimulating effect of low micromolar doses of GSH on the lectin-induced aggregation was similar to those previously reported by Essex and Li for ADP and collagen, natural platelet agonists (Essex and Li 2003).

Another level of differences between lectins was revealed with respect to the formation of HSR contacts between aggregated platelets, as it was detected by recording aggregate dissociation in response to haptenic sugars. Con A (10 μg/ml) and SNA (75 μg/ml) induced formation of very stable cell aggregates ($R = 100\%$) during several minutes, which were resistant to 60 mM α-MM and 60 mM lactose, respectively (Fig. 1c, d). This stability was sustained in the presence of micromolar doses of GSH. Platelet aggregates induced by WGA (10 μg/ml) were partly dissociated in the presence of specific haptenic sugar GlcNAc (100 mM) with $R = 82.7 \pm 3.8\%$ ($n = 5$). However, GSH significantly ($P < 0.05$) enhanced the stability of the WGA-induced aggregates, raising R to $97.6 \pm 1.7\%$ ($n = 4$) at concentration of 2.5 μM. Of interest, GSH at micromolar doses stabilized WGA-induced aggregates even if added at a maximum of aggregation response, i.e., acting as a trigger of HSR contacts (data not shown). Thus, Con A and SNA induced the formation of more stable platelet aggregates in comparison with WGA, which could result from variations in Ca^{2+}-independent transmembrane signaling in this case.

More impressive differences between lectin-induced responses of human platelets were observed when we turned to the high millimolar concentrations of GSH in the range of 0.5–6 mM. These experiments were performed with increased concentrations of lectins (10 μg/ml WGA and 100 μg/ml Con A), since we expected inhibition of platelet aggregation. At these conditions, WGA-induced platelet aggregates were relatively resistant to GlcNAc (Fig. 3a); however, there was consistent dose-dependent inhibition of WGA-induced human platelet aggregation and aggregate stability up to GSH concentration of 6 mM (Fig. 3b, c). In contrast to this gradual inhibition, a biphasic GSH dose-dependent response was observed in cases of Con A- and SNA-induced platelet aggregation, with

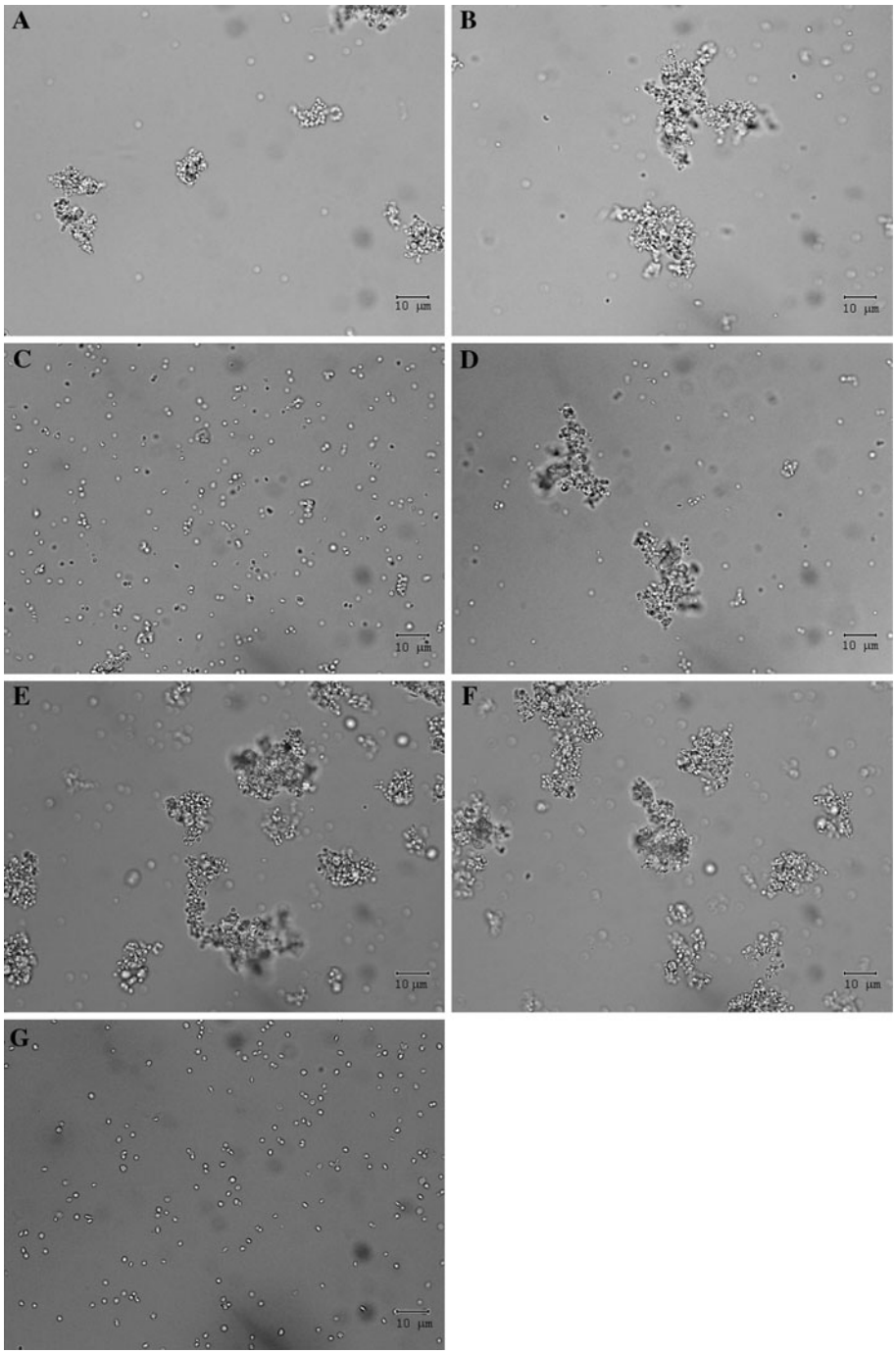

Fig. 2 Light-microscopy visualization of human platelet aggregates formed in response to WGA (5 µg/ml), Con A (10 µg/ml), and SNA (75 µg/ml) in the absence and presence of low micromolar concentration of GSH (5 µM): **a** WGA, **b** WGA + GSH, **c** Con A, **d** Con A + GSH, **e** SNA, **f** SNA + GSH, and **g** control suspension of nonaggregated human platelets. Original magnification, ×400

maximum inhibition at 3 mM and maximum stimulation at 6 mM of GSH (Fig. 3b). Of note, the stimulating effect of GSH on SNA-induced platelet aggregation significantly exceeded the relatively small change of Con A-induced response. No significant changes were observed with respect to stability of Con A- and SNA-induced aggregates as compared with GSH-untreated cells (Fig. 3c). The biphasic effect of GSH at millimolar concentrations was also confirmed by direct microscopic analysis, which revealed corresponding variations in sizes of platelet aggregates after GSH treatment (Fig. 4). While the inhibitory effect of high millimolar concentrations of GSH on platelet aggregation was predictable, as reported earlier for ADP and PAF (Pacchiarini et al. 1996), the activation of SNA-induced response was rather surprising. Because the viability of cells was sustained, the findings imply that there might be remodeling of platelet glycocalyx resulting in masking or "closing" of WGA-reactive GlcNAc residues and exposing or "opening" of SNA-reactive Neu5Acα(2,6)Gal/GalNAc residues and partly Con A-reactive α-Man/α-Glu residues,

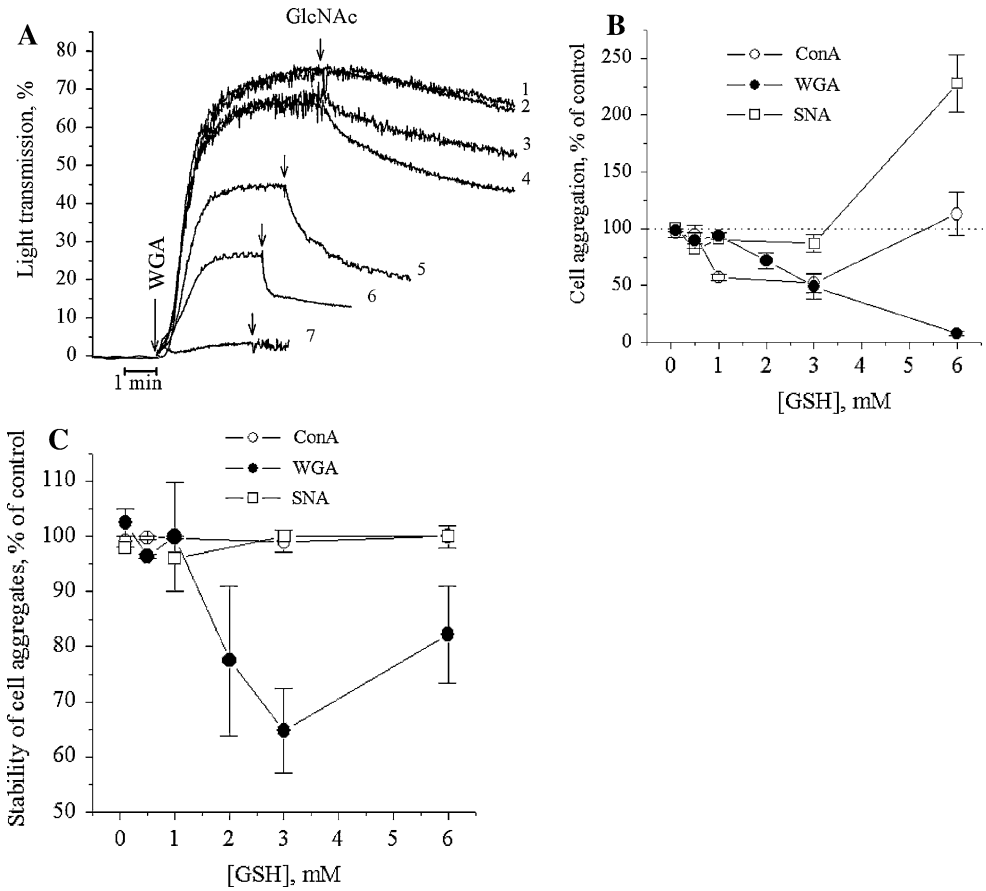

Fig. 3 Effect of GSH applied at high (millimolar) concentrations on platelet aggregation. **a** Typical kinetics of platelet aggregation induced by WGA and subsequent GlcNAc-induced disaggregation in the presence of GSH at concentrations of 0 mM (1), 0.1 mM (2), 0.5 mM (3), 1 mM (4), 2 mM (5), 3 mM (6), and 6 mM (7). The *arrows* indicate the moment of GlcNAc (100 mM) addition to the suspension of aggregated platelets. **b** Extent of lectin-induced aggregation of platelets (*T*) depending on the extracellular GSH concentration. **c** Stability of lectin-induced aggregates (*R*) depending on the extracellular GSH concentration. In all cases platelets were treated with GSH for 2 min before adding the agonists. The lectin and sugars were used at the following concentrations: 10 μg/ml WGA, 100 μg/ml Con A, 75 μg/ml SNA, 60 mM α-MM, 60 mM lactose, 100 mM GlcNAc. Each data point in **b** and **c** corresponds to mean ± SEM, $n = 3-5$

at high reducing conditions. Because this effect may be due to redox-sensitive changes of receptor clusterization (Nakashima et al. 1994; Beppu et al. 2001), resulting from remodeling of cell cytoskeleton, we next examined the effects of GSH on human platelet morphology and elastic properties using AFM.

Morphological changes of human platelets in response to GSH and cell stiffness

Treatment of human platelets with three concentrations of GSH (5 μM, 3 mM, 6 mM) which differently affected lectin-induced platelet aggregation led to significant and characteristic changes in the fine structure of the plasma membrane. Thus, in the presence of millimolar concentrations of GSH (3 mM, 6 mM), platelets appeared more heterogeneous, forming numerous blebs, filopodia, and extensions in comparison with control disk-shaped resting platelets and platelets treated with 5 μM GSH (Fig. 5). To assess the platelet surface elastic properties and cell stiffness, we determined the local Young's modulus for intact human platelets and platelets treated with GSH (Table 1). The Young's moduli of the fixed human platelets were in the range 60–170 MPa, which was approximately 1,000 times higher than for living human platelets (1–50 kPa) adhered to glass (Radmacher et al. 1996). GSH at concentrations of 5 μM and 3 mM caused decrease of Young's modulus values by approximately 40% and 10%, respectively, while GSH at concentration of 6 mM led to a notable increase of local Young's modulus by 3 times in comparison with intact platelets. These data indicate that highly reducing conditions stabilize and increase the mechanical stiffness of human platelets, while lowering the redox buffer makes cells "softer," a biphasic change which has not been previously described.

There may be several ways by which GSH can modulate morphological and mechanical properties of human platelets. In particular, cell stiffness can be changed due to redox-mediated remodeling of the cytoskeleton (Wu et al. 1998; Dalle-Donne et al. 2001, 2003; Kasas et al. 2005; Oberleithner et al. 2009) or depolarization of plasma membrane (Heinemann and Hoshi 2006; Callies et al. 2009). These mechanisms are supported by findings that pore-forming protein streptolysin O increases the elasticity of platelets, while actin cytoskeleton-stabilizing drug phalloidin partially restores the elasticity (Walch et al. 2000). Whatever biophysical mechanism is responsible for GSH-mediated modulation of platelet stiffness, it would very likely affect the state of surface glycocalyx, which contributes significantly to the adhesive behavior of cells

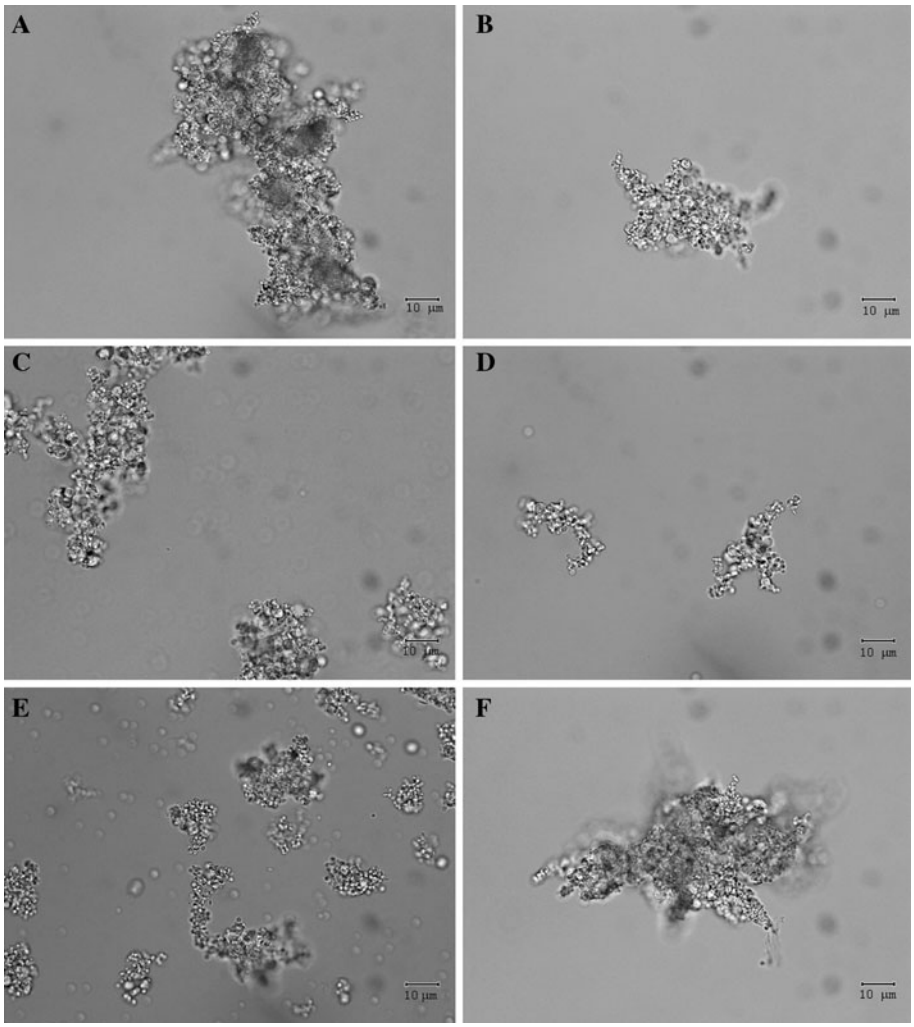

Fig. 4 Light-microscopy visualization of human platelet aggregates formed in response to WGA (10 µg/ml), Con A (100 µg/ml), and SNA (75 µg/ml) in the absence and presence of high millimolar concentration of GSH: **a** WGA, **b** WGA + 3 mM GSH, **c** Con A, **d** Con A + 3 mM GSH, **e** SNA, and **f** SHA + 6 mM GSH. Original magnification, ×400

(Agrawal and Radhakrishnan 2007). Taking into account that GSH at high doses caused a large increase of platelet stiffness, it is possible that changes in platelet morphology and stiffness mediated by GSH at millimolar concentrations reflect stabilization of cortical actin cytoskeleton, which in turn leads to different glycoligand surface exhibition and as a consequence to different platelet aggregation activity in response to various lectins. The decrease in platelet stiffness induced by GSH at micromolar concentrations may be due to disorganization of actin cytoskeleton. It is known that cortical actin cytoskeleton exerts a negative regulatory role on store-mediated calcium entry (Rosado et al. 2000, 2004). As GSH at micromolar concentrations potentiated platelet aggregation induced by agonists which trigger intracellular Ca^{2+} signaling, it is intriguing to speculate that GSH at micromolar concentrations enhances platelet aggregation via Ca^{2+}-dependent reorganization of actin cytoskeleton.

Thus, low and high concentration of GSH affected differently, often oppositely, the platelet stiffness and lectin-induced aggregation of human platelets, and these differences become more challenging when the carbohydrate-binding specificity of lectins was considered. The biphasic effects of GSH are a common theme of many studies, although the particular mechanisms may vary significantly. For instance, GSH at micromolar concentrations is known to serve as a substrate for protein disulfide oxidoreductases, leading to functional sulfhydryl rearrangements of membrane proteins and glutathionylation, while GSH at millimolar concentrations possibly leads to formation of high reduction potential that nonselectively alters protein thiols/disulfides and thus their function (Essex 2009; Ghezzi 2005). In this context, it should be noted that effects of GSH can be interpreted not only in terms of concentrations but also in terms of redox potentials of the GSSG/2GSH couple according to the Nernst equation (refer to the "Materials and methods" section). Because higher GSH concentrations reduce the extracellular redox potential and increase the redox buffering capacity of the medium, we decided to perform a quantitative analysis of these factors as prospective regulators of cell aggregation.

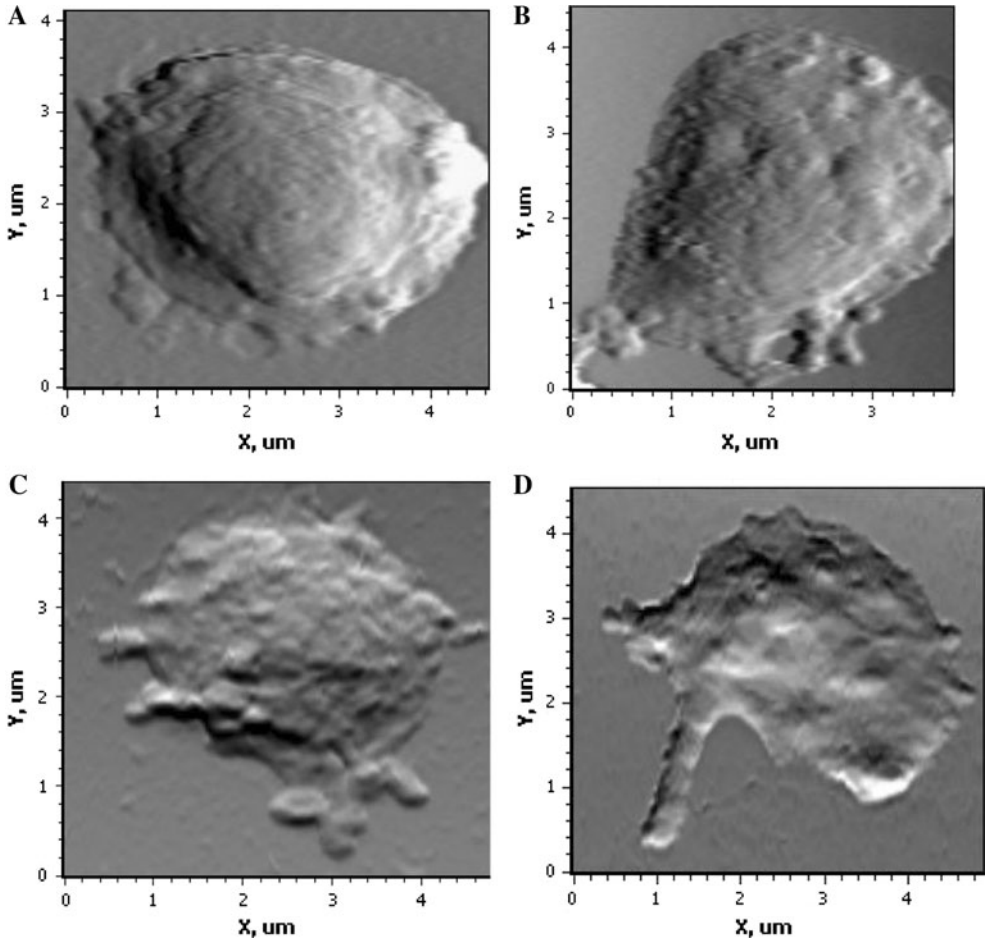

Fig. 5 Atomic force microscopy images of human platelets in the presence of GSH. Before imaging, PRP was treated with different concentrations of GSH for 10 min at room temperature and then fixed with 1.5% glutaraldehyde for 30 min: **a** an intact platelet, **b** 5 μM GSH, **c** 3 mM GSH, and **d** 6 mM GSH. Scanning area sizes are 4.6 × 4.1 μm (**a**), 3.8 × 4.5 μm (**b**), 4.8 × 4.4 μm (**c**), and 4.9 × 4.6 μm (**d**)

Table 1 Effects of GSH on surface elasticity of human platelets

Intact cells	5 μM GSH	3 mM GSH	6 mM GSH
61.0 ± 5.6	42.6 ± 3.5*	56.2 ± 7.1	191.6 ± 7.0**

Average ± SEM values of Young's modulus (*E*, MPa) at indentation depth of 25 nm are presented

* $P < 0.01$; ** $P < 0.001$ in comparison with control untreated cells

Extracellular redox potential controls human platelet aggregation

Platelet plasma membrane is poorly permeable to glutathione, which allows for easy manipulation of extracellular redox potentials by varying the concentration of GSSG/2GSH redox couple components in cell suspension. As WGA- and SNA-mediated reactions demonstrated opposite trends in response to treatments with GSH, we selected these two lectins for our experiments with redox potentials.

First, the aggregation of human platelets was induced by WGA (10 μg/ml) in media with three different constant concentrations of (GSH + 2GSSG) of 5 μM, 100 μM, and 3 mM. These conditions correspond to the fixed buffering capacity of the GSSG/2GSH redox couple. Changing the extracellular redox potential from approximately −250 to 0 mV led to either a decrease or increase in WGA-induced aggregation of human platelets depending on the redox buffer (Fig. 6). Voltage-dependent decrease of both WGA-induced cell aggregation and the stability of cell aggregates was observed in the presence of low total glutathione concentration of 5 μM (Fig. 6a), whereas voltage-dependent increase was clearly observed in the presence of high total glutathione concentration of 3 mM (Fig. 6c). At total glutathione concentration of 100 μM, the significance of redox potential was less evident (Fig. 6b), indicating that the balance between redox-potential-dependent and redox-potential-independent effects of glutathione might be important. We noticed no differences in trends describing the changes of the extent of aggregation (parameter *T*) and

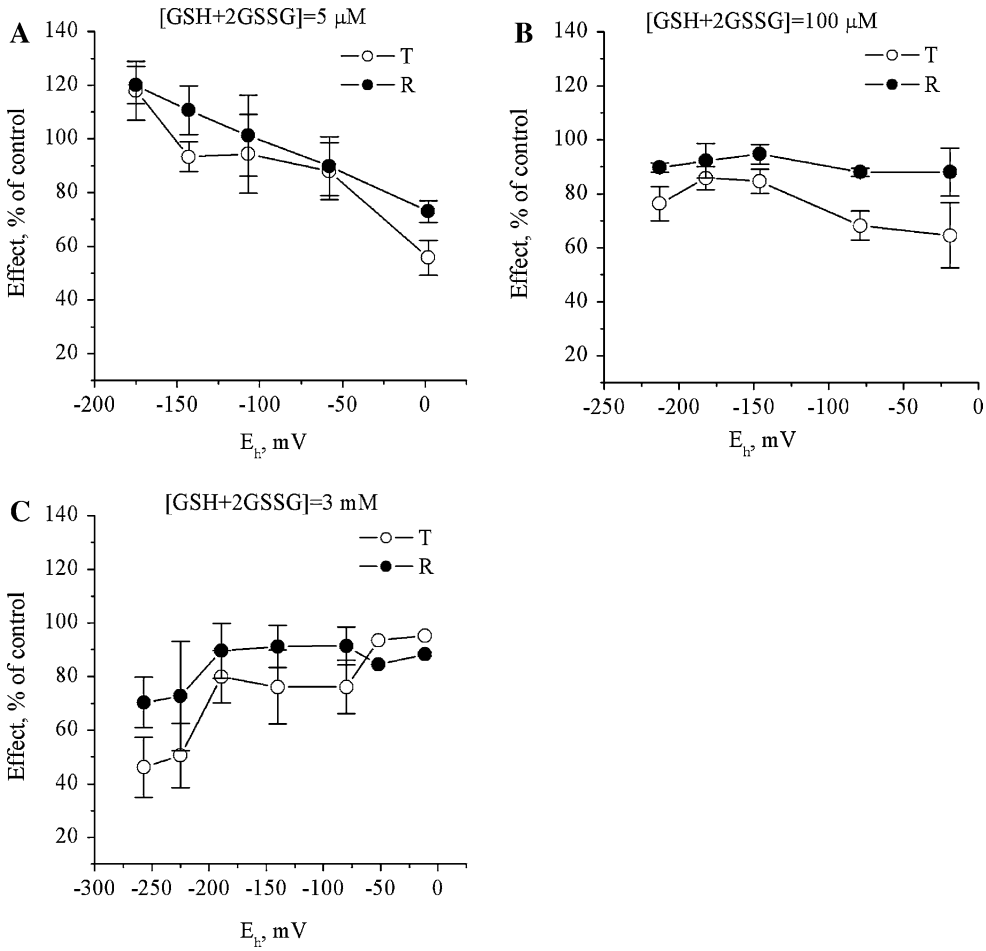

Fig. 6 Effect of the extracellular GSSG/2GSH redox potential on WGA-induced aggregation of human platelets. The extent of platelet aggregation (*T*) and the stability of lectin-induced aggregates (*R*) were calculated as described in the "Materials and methods" section. The GSH to 2GSSG ratio varied from 1:100 to 100:1, while the total concentration of (GSH + 2GSSG) was kept constant, corresponding to different redox buffering capacities of the medium, i.e., 5 μM (**a**), 100 μM (**b**), and 3 mM (**c**). Platelets were exposed to the mixture of GSH and GSSG for 2 min, and aggregation was induced by WGA at concentration of 10 μg/ml, while dissociation of cell aggregates was induced by GlcNAc at concentration of 100 mM. Each data point corresponds to mean ± SEM, $n = 3-5$

the stability of aggregates (parameter *R*), which correlated significantly with each other ($r = 0.858$, $P < 0.0001$, $n = 17$). It appeared that the glutathione redox potential damped the WGA-induced aggregation of human platelets to certain intermediate level as far as redox conditions change from reducing to oxidizing state.

Second, aggregation of human platelets was induced by SNA (75 μg/ml) in media with three different constant concentrations of (GSH + 2GSSG) of 5 μM, 100 μM, and 6 mM. Changing the extracellular redox potential from approximately −250 to 0 mV did not affect SNA-induced platelet aggregation when the total glutathione concentration was 5 or 100 μM, while led to a considerable decrease of SNA-mediated cell aggregation in the presence of total glutathione concentration of 6 mM (Fig. 7). Thus, SNA-reactive glycoligands of the plasma membrane of human platelets are masked when the extracellular redox potential increases. This change is opposite to the unmasking of WGA-reactive glycoligands at similar conditions as described above. It should be noted that, while glutathione-mediated changes of platelet aggregation at low redox buffering conditions may be due to both redox-potential-dependent and redox-potential-independent effects of glutathione, observed differences at high redox buffering conditions might be controlled predominantly by the extracellular redox potential, confirming our hypothesis about redox sensitivity of plasma membrane glycocalyx.

To the best of our knowledge, this is the first evidence that redox potential and redox buffering capacity of glutathione are factors that can control lectin-mediated cell–cell interactions and can change the expression profile and accessibility of specific glycoligands on the cell surface. Although we do not offer a mechanism explaining the redox-mediated changes of the glycocalyx at this point, we believe that the conformational flexibility of complex oligosaccharides (DeMarco and Woods 2008) might be crucial in this context. We may not also exclude redox-mediated regulation of activity of certain glycosidases (e.g., hyaluronidase and neuraminidase), which can remodel the glycocalyx (Lydataki et al. 2003). Further studies are required to find out how extracellular redox potential modulates the glycobiological properties of human platelets, i.e., the expression and accessibility of different glycoligands on the cell surface.

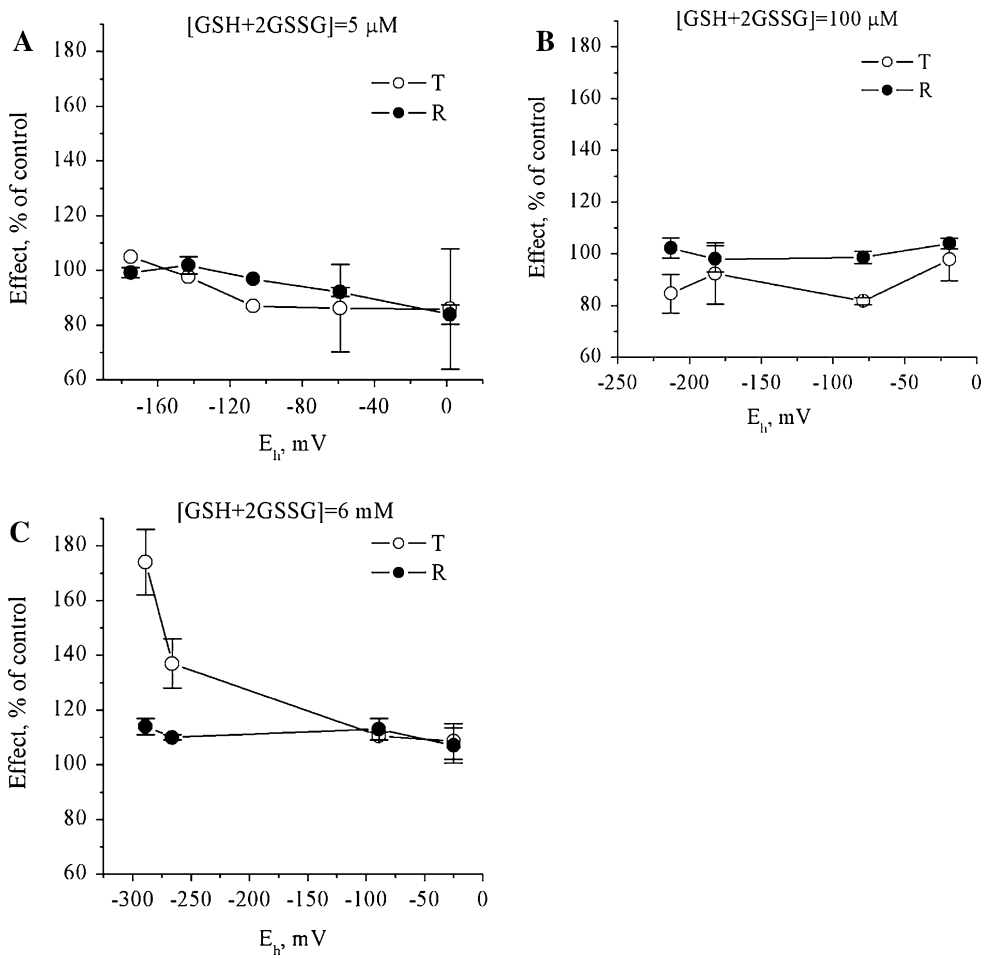

Fig. 7 Effect of the extracellular GSSG/2GSH redox potential on SNA-induced aggregation of human platelets. The extent of platelet aggregation (*T*) and the stability of lectin-induced aggregates (*R*) were calculated as described in the "Material and methods" section. The GSH to 2GSSG ratio varied from 1:100 to 100:1, while the total concentration of (GSH + 2GSSG) was kept constant, corresponding to different redox buffering capacities of the medium, i.e., 5 μM (**a**), 100 μM (**b**), and 6 mM (**c**). Platelets were exposed to the mixture of GSH and GSSG for 2 min, and aggregation was induced by SNA at concentration of 75 μg/ml, while dissociation of cell aggregates was induced by lactose at concentration of 60 mM. Each data point corresponds to mean ± SEM, $n = 3-5$

Intracellular glutathione redox status is essential for lectin-induced aggregation of human platelets

In comparison with cell surface glycocalyx (the exoplasmic face), the cytoplasmic face of the platelet membrane is exposed to highly reducing conditions, since the intracellular level of GSH is relatively high and normally maintained at the millimolar level (Essex 2009). Indeed, treatment of human platelets with 1 mM GSH did not change the intracellular level of GSH in comparison with control (Fig. 8a, inset), indicating autonomy from intracellular redox. To change glutathione-controlled intracellular redox status of human platelets, we used three cell-membrane-permeable reagents with different modes of redox activity including a sulfhydryl alkylating reagent NEM (Hansen and Winther 2009), an oxidative stress inducer menadione (Timoshenko et al. 1996), and a GSH-depleting agent diethyl maleate (DEM) (Boyland and Chasseaud 1967). All three of these reagents were found to decrease the level of intracellular GSH as detected by fluorometric assay using mBCl (Fig. 8a), which implies change of intracellular redox status from reducing to oxidative state. This forced shift of intracellular redox state resulted in uniform inhibition of lectin-induced aggregation independently of lectin type (WGA or SNA). Typical aggregation curves are shown in Fig. 8b and exemplify the dose-dependent inhibition of WGA-induced cell aggregation by DEM. Both the aggregation extent (*T*) and the stability of cell aggregates (*R*) were significantly decreased in the presence of NEM (50 μM), menadione (50 μM), or DEM (25 mM) for WGA- and SNA-mediated responses (Fig. 8c, d). Thus, the intracellular redox state seems to control the general functional ability of human platelets to aggregate in response to different agonists and to play a more robust role than the extracellular redox state. Indeed, the redox reagents used can actually work through many GSH-dependent and GSH-independent mechanisms, engaging, e.g., reactive oxygen species and multiple redox-sensitive regulatory proteins and enzymes (Essex 2009). Nevertheless, the significance of the intracellular redox status is evident, and more work should be done to understand better how it links to the extracellular redox potential.

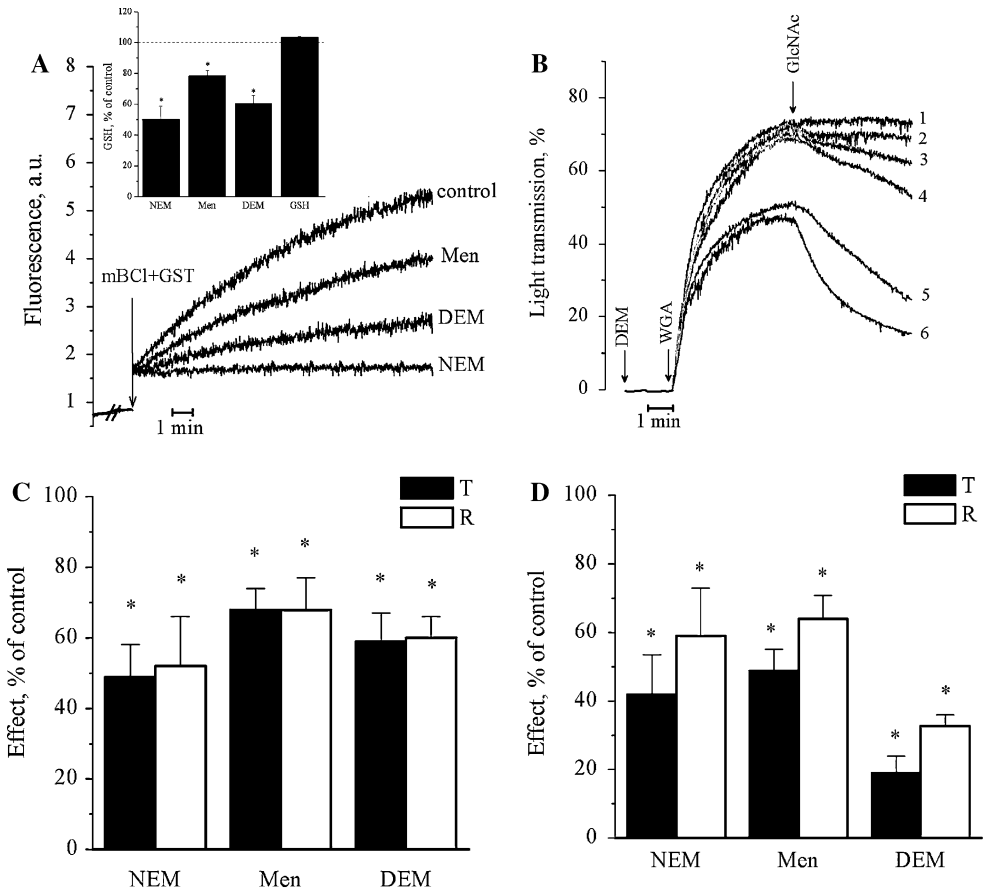

Fig. 8 Effect of redox compounds on intracellular GSH and platelet aggregation. **a** Fluorescence measurements of GSH levels in human platelets (2.5×10^8 cells/ml) using mBCl. Cells were pretreated for 5 min with 50 μM menadione (Men), 25 mM DEM, 50 μM NEM, or 10 min with 1 mM GSH and exposed to the reaction mixture containing 80 μM mBCl, 0.2% Triton X-100, and 0.24 U/ml bovine glutathione S-transferase in PBS. The increase in fluorescence (emission at 490 nm, excitation at 394 nm) is proportional to the amount of GSH-bimane adducts representing intracellular concentration of GSH. The *inset* shows the relative levels (mean ± SD) of GSH in cells recalculated from fluorescence kinetics, $*P < 0.005$, $n = 3$. **b** Typical kinetics of platelet aggregation induced by WGA (10 μg/ml) and cell aggregate dissociation induced by GlcNAc (100 mM) in the absence of DEM (1) and in the presence of DEM at concentrations of 3 mM (2), 6 mM (3), 12 mM (4), 24 mM (5), and 48 mM (6). The time points of adding DEM, WGA, and GlcNAc are indicated by arrows. **c** and **d** Effects of NEM (50 μM), menadione (50 μM, Men), and DEM (25 mM) on platelet aggregation induced by either WGA (10 μg/ml) or SNA (75 μg/ml). The extent of platelet aggregation (*T*) and the stability of lectin-induced aggregates (*R*) were calculated as described in the "Materials and methods" section. Each *bar* corresponds to mean ± SEM, $n = 3$; $*P < 0.05$ in comparison with untreated cells

Conclusions

Redox regulation of functional activity of animal and human cells represents an important biophysical mechanism beyond cell aggregation and cell–cell interactions. The results of the present study provide the first experimental evidence that glutathione as a redox molecule can affect the mechanical stiffness of human platelets and change the cell surface glycocalyx, resulting in specific modulation of lectin-induced aggregation of these cells. These effects of glutathione are biphasic and readily depend on the redox potential and redox buffering capacity of the GSSG/2GSH couple. Although our study was limited to human platelets, we believe that redox sensitivity of cellular glycocalyx is a more universal phenomenon that may open up new avenues of research in cell biophysics and glycobiology. Further work is required to unravel molecular mechanisms of redox-mediated remodeling of the cell surface glycocalyx.

References

Agrawal NJ, Radhakrishnan R (2007) The role of glycocalyx in nanocarrier-cell adhesion investigated using a thermodynamic model and Monte Carlo simulations. J Phys Chem C Nanomater Interfaces 111:15848–15856

Andre P, Capo C, Benoliel AM, Bongrand P, Rouge F, Aubert C (1990) Splitting cell adhesiveness into independent measurable parameters by comparing ten human melanoma cell lines. Cell Biophys 17:163–180

Ball C, Vijayan KV, Nguyen T, Anthony K, Bray PF, Essex DW, Dong JF (2008) Glutathione regulates integrin $\alpha_{IIb}\beta_3$-mediated cell adhesion under flow conditions. Thromb Haemost 100:857–863

Beppu M, Yokoyama N, Motohashi M, Kikugawa K (2001) Enhanced adhesion of oxidized mouse polymorphonuclear leukocytes to macrophages by a cell-surface sugar-dependent mechanism. Biol Pharm Bull 24:19–26

Bhadriraju K, Hansen LK (2002) Extracellular matrix- and cytoskeleton-dependent changes in cell shape and stiffness. Exp Cell Res 278:92–100

Boyland E, Chasseaud LF (1967) Enzyme-catalysed conjugations of glutathione with unsaturated compounds. Biochem J 104:95–102

Burch PT, Burch JW (1987) Alterations in glutathione during storage of human platelet concentrates. Transfusion 27:342–346

Callies C, Schon P, Liashkovich I, Stock C, Kusche-Vihrog K, Fels J, Strater AS, Oberleithner H (2009) Simultaneous mechanical stiffness and electrical potential measurements of living vascular endothelial cells using combined atomic force and epifluorescence microscopy. Nanotechnology 20:175104 (8 p)

Chizhik SA, Huang Z, Gorbunov VV, Myshkin NK, Tsukruk VV (1998) Micromechanical properties of elastic polymeric materials as probed by scanning force microscopy. Langmuir 14:2606–2609

Dalle-Donne I, Rossi R, Milzani A, Di Simplicio P, Colombo R (2001) The actin cytoskeleton response to oxidants: from small heat shock protein phosphorylation to changes in the redox state of actin itself. Free Radic Biol Med 31:1624–1632

Dalle-Donne I, Giustarini D, Rossi R, Colombo R, Milzani A (2003) Reversible S-glutathionylation of Cys 374 regulates actin filament formation by inducing structural changes in the actin molecule. Free Radic Biol Med 34:23–32

DeMarco ML, Woods RJ (2008) Structural glycobiology: a game of snakes and ladders. Glycobiology 18:426–440

Drozd ES, Chizhik SA (2008) Combined atomic force microscopy and optical microscopy measurements as a method of erythrocyte investigation. Proc SPIE 7377:73770E. doi:10.1117/12.836481

Essex DW (2009) Redox control of platelet function. Antioxid Redox Signal 11:1191–1225

Essex DW, Li M (2003) Redox control of platelet aggregation. Biochemistry 42:129–136

Fritz M, Radmacher M, Gaub HE (1994) Granula motion and membrane spreading during activation of human platelets imaged by atomic force microscopy. Biophys J 66:1328–1334

Ghezzi P (2005) Regulation of protein function by glutathionylation. Free Radic Res 39:573–580

Gorudko IV, Buko IV, Cherenkevich SN, Polonetsky LZ, Timoshenko AV (2008) Lectin-induced aggregates of blood cells from patients with acute coronary syndromes. Arch Med Res 39:674–681

Hansen RE, Winther JR (2009) An introduction to methods for analyzing thiols and disulfides: reactions, reagents, and practical considerations. Anal Biochem 394:147–158

Hartwig JH (2006) The platelet: form and function. Semin Hematol 43:94–100

Heinemann SH, Hoshi T (2006) Multifunctional potassium channels: electrical switches and redox enzymes, all in one. Sci STKE 2006:pe33. doi:10.1126/stke.3502006pe33

Higashihara M, Takahata K, Ohashi T, Kariya T, Kume S, Oka H (1985) The platelet activation induced by wheat germ agglutinin. FEBS Lett 183:433–438

Hill TD, White JG, Rao GH (1989) The influence of glutathione depleting agents on human platelet function. Thromb Res 53:457–465

Hwang C, Sinskey AJ, Lodish HF (1992) Oxidized redox state of glutathione in the endoplasmic reticulum. Science 257:1496–1502

Jonas CR, Ziegler TR, Gu LH, Jones DP (2002) Extracellular thiol/disulfide redox state affects proliferation rate in a human colon carcinoma (Caco2) cell line. Free Radic Biol Med 33:1499–1506

Kasas S, Wang X, Hirling H, Marsault R, Huni B, Yersin A, Regazzi R, Grenningloh G, Riederer B, Forro L, Dietler G, Catsicas S (2005) Superficial and deep changes of cellular mechanical properties following cytoskeleton disassembly. Cell Motil Cytoskeleton 62:124–132

Kim SR, Lee JY, Lee MY, Chung SM, Bae ON, Chung JH (2001) Association of quinone-induced platelet anti-aggregation with cytotoxicity. Toxicol Sci 62:176–182

Kirlin WG, Cai J, Thompson SA, Diaz D, Kavanagh TJ, Jones DP (1999) Glutathione redox potential in response to differentiation and enzyme inducers. Free Radic Biol Med 27:1208–1218

Kumar A, Sharma S, Pundir CS, Sharma A (1995) Decreased plasma glutathione in cancer of the uterine cervix. Cancer Lett 94:107–111

Lydataki S, Lesniewska E, Tsilimbaris MK, Le Grimellec C, Rochette L, Goudonnet JP, Pallikaris IG (2003) Observation of the posterior endothelial surface of the rabbit cornea using atomic force microscopy. Cornea 22:651–664

Mathur AB, Collinsworth AM, Reichert WM, Kraus WE, Truskey GA (2001) Endothelial, cardiac muscle and skeletal muscle exhibit different viscous and elastic properties as determined by atomic force microscopy. J Biomech 34:1545–1553

Matsuda S, Ikeda Y, Aoki M, Toyama K, Watanabe K, Ando Y (1979) Role of reduced glutathione on platelet functions. Thromb Haemost 42:1324–1331

Moriarty-Craige SE, Jones DP (2004) Extracellular thiols and thiol/disulfide redox in metabolism. Annu Rev Nutr 24:481–509

Nakashima I, Pu MY, Nishizaki A, Rosila I, Ma L, Katano Y, Ohkusu K, Rahman SM, Isobe K, Hamaguchi M (1994) Redox mechanism as alternative to ligand binding for receptor activation delivering disregulated cellular signals. J Immunol 152:1064–1071

Oberleithner H, Callies C, Kusche-Vihrog K, Schillers H, Shahin V, Riethmüller C, MacGregor GA, Wardener HE (2009) Potassium softens vascular endothelium and increases nitric oxide release. PNAS 106:2829–2834

Pacchiarini L, Tua A, Grignani G (1996) In vitro effect of reduced glutathione on platelet function. Haematologica 81:497–502

Palumaa P (2009) Biological redox switches. Antioxid Redox Signal 11:981–983

Pastore A, Federici G, Bertini E, Piemonte F (2003) Analysis of glutathione: implication in redox and detoxification. Clin Chim Acta 333:19–39

Pidard D, Didry D, Kunicki TJ, Nurden AT (1986) Temperature-dependent effects of EDTA on the membrane glycoprotein IIb-IIIa complex and platelet aggregability. Blood 67:604–611

Radmacher M, Fritz M, Kacher CM, Cleveland JP, Hansma PK (1996) Measuring the viscoelastic properties of human platelets with the atomic force microscope. Biophys J 70:556–567

Rosado JA, Jenner S, Sage SO (2000) A role for the actin cytoskeleton in the initiation and maintenance of store-mediated calcium entry in human platelets. Evidence for conformational coupling. J Biol Chem 275:7527–7533

Rosado JA, López JJ, Harper AJS, Harper MT, Redondo PS, Pariente JA, Sage SO, Salido GM (2004) Two pathways for store-mediated calcium entry differentially dependent on the actin cytoskeleton in human platelets. J Biol Chem 279:29231–29235

Ruggeri ZM (2002) Platelets in atherothrombosis. Nat Med 8:1227–1234

Samal AB, Timoshenko AV, Loiko EN, Kaltner H, Gabius HJ (1998) Formation of lactose-resistant aggregates of human platelets induced by the mistletoe lectin and differential signaling responses to cell contact formation by the lectin or thrombin. Biochemistry (Mosc) 63:516–522

Samiec PS, Drews-Botsch C, Flagg EW, Kurtz JC, Sternberg P Jr, Reed RL, Jones DP (1998) Glutathione in human plasma: decline in association with aging, age-related macular degeneration, and diabetes. Free Radic Biol Med 24:699–704

Sharon N, Lis H (2003) Lectins, 2nd edn. Kulwer Academic, Dordrecht, p 454

Shimizu H, Kiyohara Y, Kato I, Kitazono T, Tanizaki Y, Kubo M, Ueno H, Ibayashi S, Fujishima M, Iida M (2004) Relationship between plasma glutathione levels and cardiovascular disease in a defined population. Stroke 35:2072–2077

Timoshenko AV, Zorin VP, Cherenkevich SN (1986) Effect of prostaglandins and inhibitors of arachidonic acid methabolism on concanavalin A-induced agglutination of thymocytes. Abstracts of the All-Union Symposium on Synthesis and Study of Prostaglandins at Tallinn, USSR, November 1986, 169

Timoshenko AV, Loiko EN, Cherenkevich SN, Gabius HJ (1996) Effects of metabolic inhibitors and lectins on the menadione-dependent generation of H_2O_2 by rat thymocytes. Biochem Mol Biol Int 40:1149–1158

Timoshenko AV, Gorudko IV, Cherenkevich SN, Gabius HJ (1999) Differential potency of two crosslinking plant lectins to induce formation of haptenic-sugar-resistant aggregates of rat thymocytes by post-binding signaling. FEBS Lett 449:75–78

Torti M, Festetics ET, Bertoni A, Sinigaglia F, Balduini C (1999) Clustering of integrin αIIb-β3 differently regulates tyrosine phosphorylation of pp72syk, PLCgamma2 and pp125FAK in concanavalin A-stimulated platelets. Thromb Haemost 81:124–1304

Walch M, Ziegler U, Groscurth P (2000) Effect of streptolysin O on the microelasticity of human platelets analyzed by atomic force microscopy. Ultramicroscopy 82:259–267

Wang H, Joseph JA (2000) Mechanisms of hydrogen peroxide-induced calcium dysregulation in PC12 cells. Free Radic Biol Med 28:1222–1231

Wu HW, Kuhn T, Moy VT (1998) Mechanical properties of L929 cells measured by atomic force microscopy: effects of anticytoskeletal drugs and membrane crosslinking. Scanning 20:389–397

Yan Z, Garg SK, Kipnis J, Banerjee R (2009) Extracellular redox modulation by regulatory T cells. Nat Chem Biol 5:721–723

Yang YT, Lin CC, Liao JD, Chang CW, Ju MS (2010) Continuous depth-sensing nano-mechanical characterization of living, fixed and dehydrated cells attached on a glass substrate. Nanotechnology 21:285704

Yatomi Y, Ozaki Y, Koike Y, Satoh K, Kume S (1993) Wheat germ agglutinin-induced intracellular calcium mobilization in human platelets: suppression by staurosporine and resistance to cyclic AMP inhibition. Biochem Biophys Res Commun 15:453–458